LA-UR-87-1535

TITLE: CHERENKOV AND TRANSITION RADIATION DIAGNOSTICS FOR HIGH ENERGY FREE-ELECTRON LASERS

LA-UR--87-1535

DE87 010106

AUTHOR(S): Alex H. Lumpkin, P-15

SUBMITTED TO: Proceedings for AIAA 19th Fluid Dynamics, Plasma Dynamics and Laser Conference, Honolulu, Hawaii, June 7-10, 1987

CHERENKOV AND TRANSITION RADIATION DIAGNOSTICS FOR HIGH ENERGY FREE-ELECTRON LASERS*

Alex H. Lumpkin
Los Alamos National Laboratory
Physics Division
P. O. Box 1663
Los Alamos, NM 87545 USA

Abstract

Electron Beam diagnostics based on imaging techniques using Cherenkov conversion screens and intensified video cameras should be adaptable to the developing high-energy free-electron lasers (FEL) driven by radio frequency powered linear accelerators. The high beam energies (60-150 MeV) and the peak currents (100s of amps) anticipated should also make optical transition radiation intensities sufficient for these techniques. The distinctive features of the two light generation mechanisms will be summarized and a few diagnostic examples will be cited.

Introduction

The developing high-energy free-electron lasers (FEL) based on radio frequency (RF) powered linear accelerators involve electron beam energies of 60-150 MeV, micropulse durations of 10-20 ps, and micropulse separations of 10-50 ns. These micropulses are typically in a pulse train of at least 100 μs in length.[1] The importance of understanding any structure within a micropulse has been graphically demonstrated in studies on the Los Alamos FEL as reported previously.[2] Lasing regimes within the micropulse, parameter optimization via phasing of the RF components, and beamline wakefield effects (at high peak currents) have been observed. These studies were all performed using the Cherenkov mechanism to convert the electron distribution into a visible image during the electrons' transit through fused silica screens. With the higher beam energies and peak currents it appears that transition radiation,[3] which is produced when a charged particle beam crosses a boundary between two media with different dielectric constants, can also play a role. As an example, using vacuum to metal foil transitions and electron energies as mentioned, the emitted broadband radiation includes the visible region, and therefore imaging techniques developed for Cherenkov light are applicable. The distinctive features of the two mechanisms will be summarized and a few diagnostic examples will be cited.

Picosecond-Regime Light Generation Mechanisms

In order to address phenomena on the 10-ps time scale of an electron beam micropulse, we have used both an RF deflector and a streak camera. In the first case, the time-dependent deflection of the electron beam is observed on the radiation converter screen itself and so picosecond formation processes are not necessary. However, there are few, if any, fluorescent screens that can withstand the high energy deposition from our beams and provide even nanosecond response times so that individual micropulses can be selected. Fused silica screens are damage resistant and provide sufficient light via the Cherenkov effect. In the second case, the time dependent deflection is within a streak tube itself so the conversion process at the screen must be less than the pulse duration in order to evaluate it.

Figure 1 shows an example of the variation of the electron charge distribution in energy and time as a function of the relative phase of accelerators B and A. This loss of energy <u>within</u> the micropulse is attributed to beamline wakefield effects that occur at high peak currents at beamline discontinuities.[2] Figure 2 shows an example of the measurement of the micropulse time width using a streak camera. In this case the measurement was performed after the nonisochronous 60° bend, and we used magnetic bunching to compress the pulse in time (<15 ps.). Having illustrated the use of such imaging techniques, it would be instructive to briefly review the two mechanisms under consideration: Cherenkov and Optical Transition Radiation (OTR).

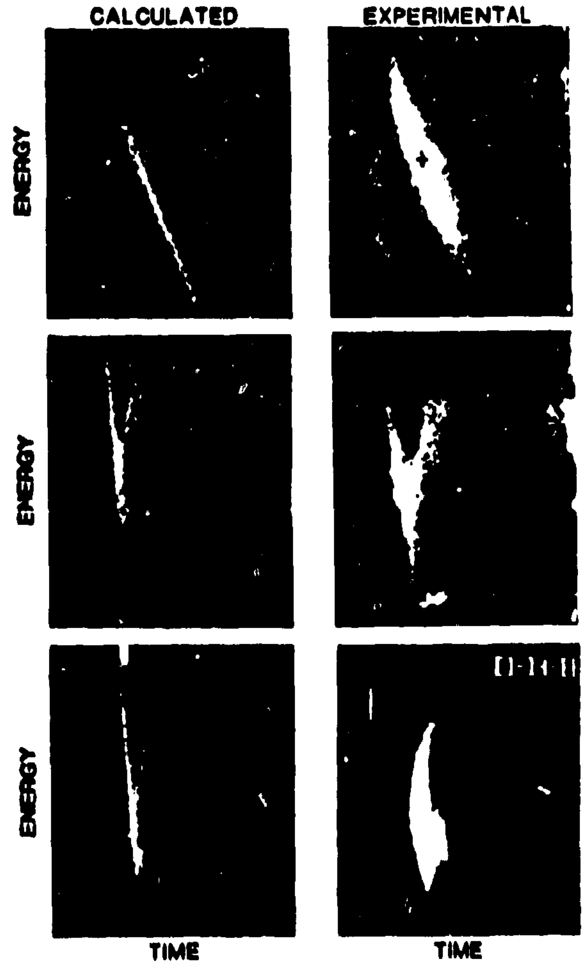

Fig. 1. A comparison of energy-time plots for calculated and experimental charge distributions.

*Work performed under the auspices of the U.S. Dept. of Energy and supported by the Department of Defense U.S. Army Strategic Defense Command.

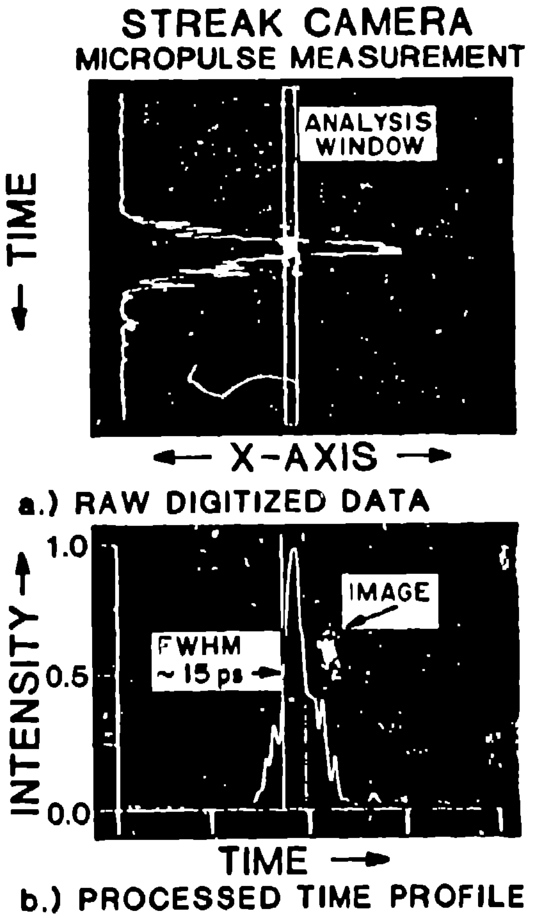

Fig. 2. Streak camera measurement of the electron beam micropulse time width, Δt ~ 15 ps full width half maximum (FWHM).

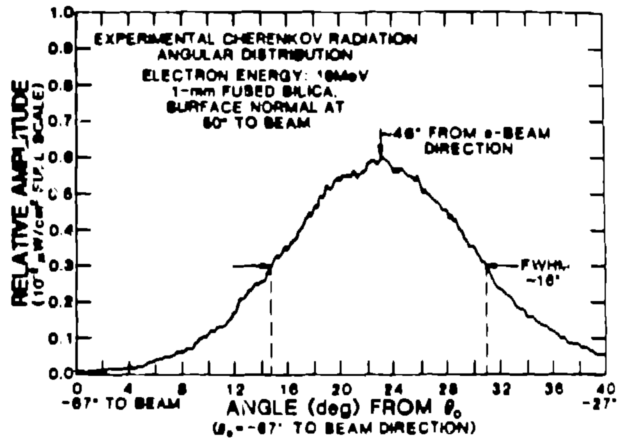

Fig. 3. Cherenkov light angular distribution measurement for a 16-MeV electron beam incident on a 1-mm-thick fused silica screen whose normal is oriented at -50° to the beam direction. The peak in the pattern is at about 46°.

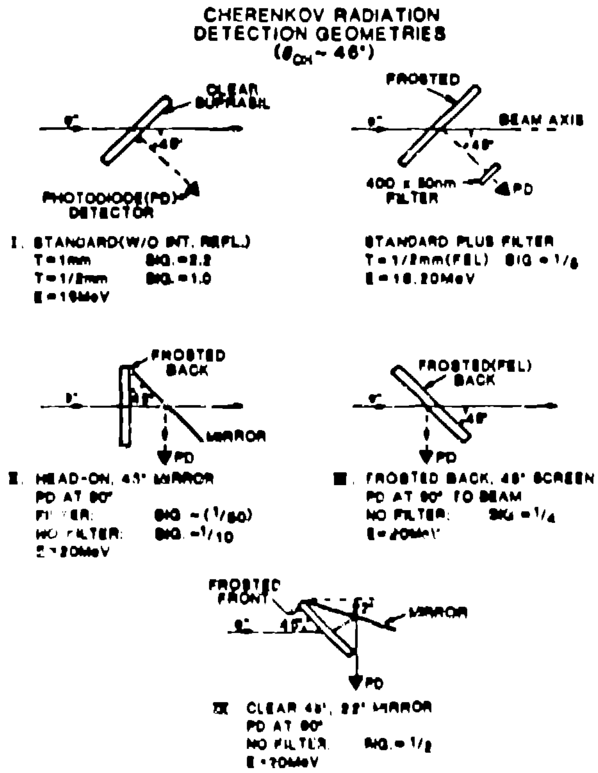

Fig. 4. Schematic presentation of several setups for Cherenkov beamline diagnostics and the observed signal relative to case I.

Cherenkov Radiation

Cherenkov light is produced when a highly relativistic charged particle with velocity $\beta = v/c \sim 1$ transits a medium with index of refraction, n, such that $\beta n > 1$. The light is emitted in a cone around the direction of electron motion at an angle $\theta = \cos^{-1} 1/\beta n$. As an example for electrons with $\beta = 0.99$ in fused silica with $n \sim 1.5$, $\theta \sim 47°$. The number of photons (N) emitted between two wavelengths λ_1 and λ_2 can be calculated by the following equation from Ref. 4:

$$N = 2\pi\alpha\ell\left(\frac{1}{\lambda_2} - \frac{1}{\lambda_1}\right)\left(1 - \frac{1}{\beta^2 n^2}\right) . \qquad (1)$$

where $\alpha = e^2/\hbar c$ the fine structure constant, ℓ is the thickness of the medium (fused silica in this case), and β and n are as above. This relation indicates that the number of photons emitted in the visible is about ten per electron per mm of silica. Also, the spectral distribution goes as $1/\lambda^3$. That is, one sees a bluish light although there is even more energy in the ultraviolet. Since the intensity and angular distribution are β-related, and β approaches one asymptotically, they might be approximated as energy independent for electron energies of $\gamma > 10$ (where γ is the Lorentz factor).

In Fig. 3 an experimental Cherenkov angular distribution from a 16-MeV electron beam incident on a 1-mm-thick fused silica screen (oriented with its normal 50° to the beam direction) is shown. These data were obtained at the EG&G (Santa Barbara) Linac facility. Finite beam diameter and divergence effects contribute to the angular spread of the emission cone. Figure 4 schematically shows several setups for using Cherenkov light as a beamline diagnostic and the effect on signal intensity. At our FEL facility we have used a frosted back surface to break-up the Cherenkov cone and obtain sufficient signal at 90° to the beam direction. Geometry II (normal incidence) is important because the light does not scatter within the silica screen as much as it does in the downstream direction for the 45° orientation.

Transition Radiation

Transition radiation is produced by a moving charged particle at the interface of two media with different dielectric constants. It is broadband (microwave to x-ray), but I will deal only with the optical transition radiation (OTR).[3,5] Its distinctive features illustrated in Figs. 5-7 include an intensity and angular distribution which are strong functions of the energy of the producing particle (in contrast to Cherenkov radiation), a broad spectrum which shows a $1/\lambda^2$ dependence with an upper limit proportional to γ (conversion efficiency is only 1 photon per 100 electrons per interface at $\gamma \sim 40$), strong polarization of the electric vector, and of course, a prompt (few ps) production time. When an electron crosses a finite foil thickness, there are two interfaces and both forward and backward radiation result. For normal incidence of relativistic electrons these radiation patterns are peaked within a degree, $\theta_p \sim 1/\gamma$, from the surface normals. One of the more interesting features is that for a foil at 45° to the beam direction the forward radiation is the same, but the backward radiation is emitted in a thin cone around the direction of specular reflection, i.e., at 90° ± θ_p to the beam direction,[3-5] (see Figs. 5 and 6). This latter features makes

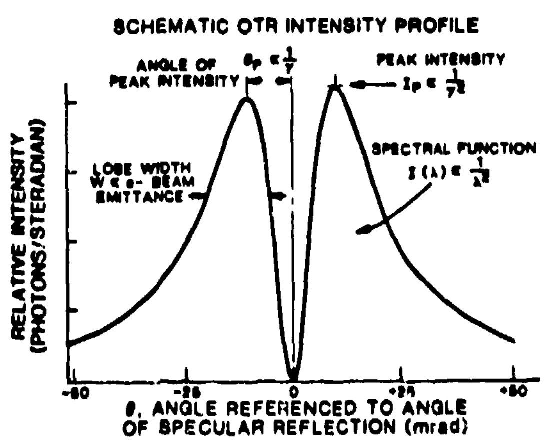

Fig. 5. Schematic illustration of OTR intensity profile parameters' dependence on γ or beam divergence. Shown are the peak intensity, angle of the lobe, and lobe width.

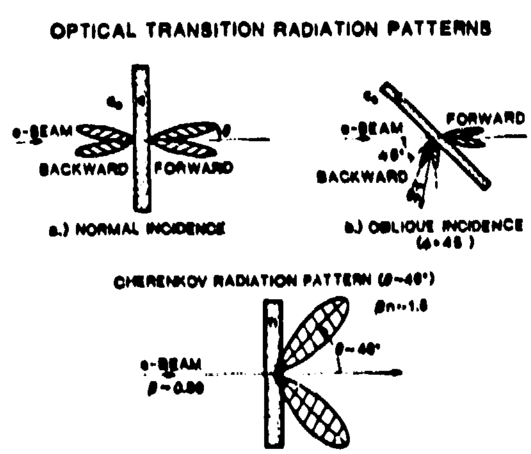

Fig. 6. Schematic illustration of the OTR forward and backward radiation for cases of the beam-incident normal and obliquely to the foil.

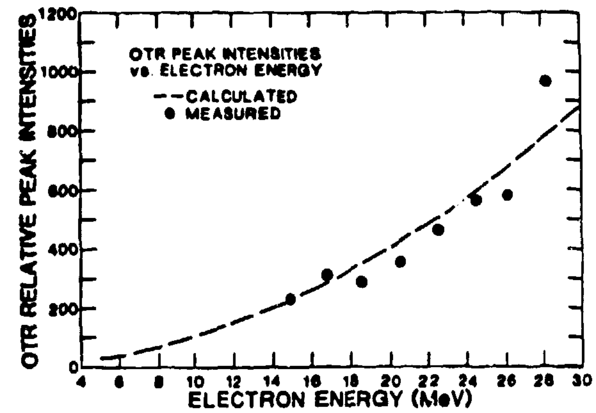

Fig. 7. Comparison of experimental and calculated OTR peak intensity as a function of beam energy (from Reference 6).

it very practical for beamline imaging diagnostics. As noted above, the low conversion efficiency (0.01 photons per electron, per interface) is a disadvantage relative to Cherenkov radiation. However, its angular distribution is so much more concentrated than the Cherenkov cone from fused silica that at 90° to the beam the photon intensity should be adequate. It has been detected and characterized under certain conditions.[3,5,6] Also, as shown in Fig. 7, the peak intensity increases as γ^2 so that for $\gamma > 40$ there should be even more signal.[6]

Comments on Potential Electron Beam Diagnostic Applications

Electron Beam Position And Profile Measurements

These are routinely performed at the Los Alamos facility with 0.5-mm-thick fused silica screens normal to the beam (frosted back surface) and a polished metal mirror at 45° to the beam positioned behind the screen that directs the Cherenkov light out the 90° port. This is not the optimum geometry for the Cherenkov cone and single micropulses (100 A peak) are just seen with an intensified camera. If the fused silica screens are rotated at 45° to the beam, the Cherenkov light tends to internally reflect in the downstream direction within the screen and significantly spread the spot. However, a metal foil for the OTR generation should only exhibit the $\sqrt{2}$ spreading of the beam spot due to the 45° angle and this is canceled by viewing at 90° to the beam direction. Subject to foil survivability this could be an excellent alternative technique. In fact, visible radiation from a polished Molybdenum (Moly) foil has been observed in our laboratory in one of our standard beamline positions. This radiation intensity was comparable to that from the fused silica screen plus metal mirror when viewed at 90° to the beam direction (see Fig. 8). The detected intensity dropped off rapidly with misalignment of the foil from 45° to the beam and disappeared in less than one microsecond after the end of the pulse train. A gated intensified camera was used to sample about 400 ns of the 50 to 100 μs-long macropulse's interaction with the converter screen or foil. When viewing the scene with the gated camera, the radiation intensity from the foil sampled at the end of the macropulse did not appear to vary with the length of the macropulse (as might be expected from incandescence). These features are consistent with OTR, but further experiments are planned.

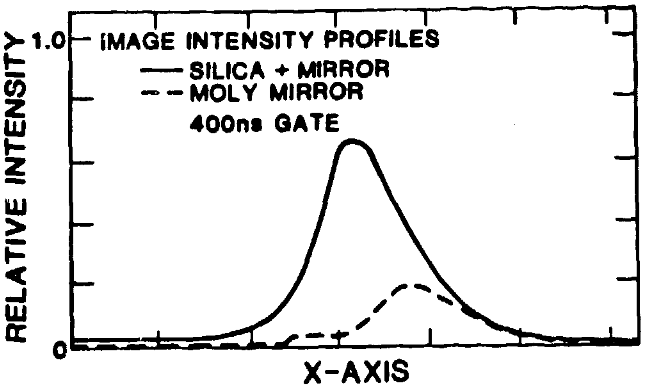

Fig. 8. Observed signals at 90° to the 20-MeV electron beam direction from a fused silica screen plus Moly metal mirror and a Moly metal foil alone.

Electron Beam Emittance

At Los Alamos, we currently evaluate the 20-MeV electron beam emittance by observation (Cherenkov light) of the beam size (profile) as a function of a focusing quadrupole field variation or by evaluating the beam diameter at two separate locations under fixed focusing conditions. Recently, it has been reported the emittance can be measured by using a single OTR foil and comparing the angular distribution (the lobes) of the OTR pattern to calculated curves involving beam emittances.[5] This could be an interesting alternative technique.

Electron Beam Energy And Energy Spread

Standard procedures for evaluating electron beam energy involve an electron spectrometer with its analyzing magnet and focal plane detector. We normally use fused silica screens in the focal plane and record the energy distribution for a few micropulses with intensified television cameras. With our current geometry we probably could put a foil in the focal plane, but because the OTR intensity is energy and incident angle dependent, there would be an involved calibration procedure. Alternatively, single foil techniques are expected to provide ~ 3 per cent energy resolution[5] and two-foil interferometric OTR techniques have yielded ~ 1 percent energy resolution at $\gamma = 100$[3]. These techniques would allow energy measurements along the beamline (between accelerator sections) as desired without installation of an analyzing magnet and spectrometer chamber (a potential wakefield source).

Electron Beam Temporal Profile

The temporal pulse width of a micropulse of 10-20 ps duration can be evaluated using a streak system (a streak camera or an RF deflector)[2] if the light generation mechanism is only a few picoseconds. The conversion efficient Cherenkov mechanism has the advantage in intensity, but OTR may be usable at the higher energies (peak intensity goes as γ^2) and peak currents. Also, limiting the effective spatial extent of the generated light reduces the corresponding time spread so that OTR foils might have an advantage in this aspect over Cherenkov screens.

Summary and Conclusion

In summary, light generation mechanisms that are on the picosecond timescale can be used for diagnostics of electron beam micropulses or macropulses via imaging techniques. It appears that transition radiation diagnostics may provide an interesting and valuable complement to Cherenkov radiation diagnostics for emerging high energy FEL systems. In the case of beam position (profile) and temporal profiles the techniques may already be established. For electron beam energy and emittance measurements further work is needed. Also, there are indications that OTR polarization effects could be exploited to improve diagnostic sensitivity for some of these parameters. This issue should certainly be explored in the future.

Acknowledgements

The author is indebted to Paul Zagarino, Steve Iverson, and Charles Iverson of the EG&G, Santa Barbara, Linac facility staff for discussing possible OTR applications to FELs; for assisting in the Cherenkov radiation measurements; and for providing preliminary OTR data (S.I.).

References

[1] Section I and VI, Proceedings of the Seventh International Conference on Free-Electron Lasers, Tahoe City, California, Sept. 8-13, 1985, Nucl. Inst. and Methods, Vol. A250, Nos. 1 and 2.

[2] A.H. Lumpkin and D.W. Feldman, "Diagnostics of the Los Alamos Free-Electron Laser Using Streak Systems," Proceedings of the Eighth International Free-Electron Laser Conference, Glasgow, Scotland, Sept. 1-5, 1986, LA-UR-86-2984.

[3] L. Wartski, et. al., "Interference Phenomenon in Optical Transition Radiation and Its Application to Particle Beam Diagnostics," Journal of Applied Physics, Vol. 46, No. 8, August 1975, p. 3644.

[4] J.V. Jelley, Cherenkov Radiation and Its Applications, Pergamon Press (1958).

[5] R.B. Fiorito, et. al., "Transition Radiation Diagnostics for Intense Charged Particle Beams," Proceedings of the Sixth International Conference on High Power Beams, Kobe, Japan, 1986. To be published in Journal of Lasers and Particle Beams.

[6] S. Iverson (EG&G - Goleta), private communication, July 1985. Also, Project Summary: Los Alamos National Laboratory Support Program, (July-September 1985), EG&G (Santa Barbara Operations), EG&G 10282-2086, October 1985, p. 9.